

Figure 1 Variation of relative tensile modulus (E_c/E_p) of PP/Ag (open symbols untreated and closed symbols treated) composites with volume fraction of filler ϕ_F . The solid curves A and B represent the upper bound equation and lower bound equation, respectively [eq. (1) and (2)]. The dashed curve C represents variation of data.

obtained from Kenrich Petrochemical Inc. (Bayonne, NJ).

Surface Modification of Ag

A very low percentage (0.4 wt %) of LICA-38 on the basis of Ag powder was diluted in 200 mL distilled toluene and then mixed with Ag powder in a high speed mixer. The slurry was first dried in an oven at 373 K for 24 h and finally the coated filler was dried in a vacuum at 353 K for 12 h.

Compounding and Molding

Vacuum dried iPP and Ag powder were homogenized on a two roll mill at 433 ± 5 K for 15 min to make thin sheets of the composites with filler content of 0–5.6% (0–70 wt %) Ag. Sheets of 1 and 5 mm thickness were then compression molded from several of the primary sheets at 473 ± 5 K and 34.5 MPa pressure. The mold assembly was cooled under load by the circulation of water at a rate of 20 K/min. Dumbbell-shaped tensile specimens were machined from 1-mm thick sheets, while notched bar-type samples for Izod impact tests and bar samples for flexural tests were made from sheets of 5-mm thick molded specimens. Unfilled iPP was also processed through identical conditions of temperature and pressure and machined into the required dimensions for the studies.

Measurements

Tensile properties were measured on an Instron Universal Testing machine (Model 1121) at an ex-

tension rate of 100% (initial crosshead separation 5 cm and crosshead speed 5 cm/min) according to the ASTM D 638-82 test procedure. Flexural properties were estimated on the Instron using a three point loading fixture according to the ASTM D 790 test procedure. Izod impact strength values were evaluated on notched samples on an FIE instrument (Model IT-0.42) according to ASTM D 256 with a notch depth of 2.5 mm and a notch angle of 45° . At least five samples were tested and the average value reported. All the tests were performed at ambient temperature, 303 ± 2 K.

RESULTS AND DISCUSSION

Tensile Properties

Tensile modulus, tensile strength, and elongation at break were determined from the stress–strain curves (not shown) and are presented in Figures 1–9- as variations of the ratio of the property of the composite (subscript c) to that of the unfilled iPP (subscript p) versus volume fraction of Ag powder, ϕ_F .

Figure 1 presents the variation of relative tensile modulus (E_c/E_p) against ϕ_F . The modulus showed a drastic decrease at ϕ_F of 1.3% beyond which the decrease was only marginal. This implies that incorporation of Ag into PP forms a weak structure. This weakness may be a result of debonding of metal particles from the polymer so that even at small deformation the interphase of filler polymer create discontinuities through stress concentrations. One possible reason for this debonding or lack of interaction (or adhesion) between Ag and PP may be that PP, being a semicrystalline polymer, will always have a tendency to crystallize, which would exclude

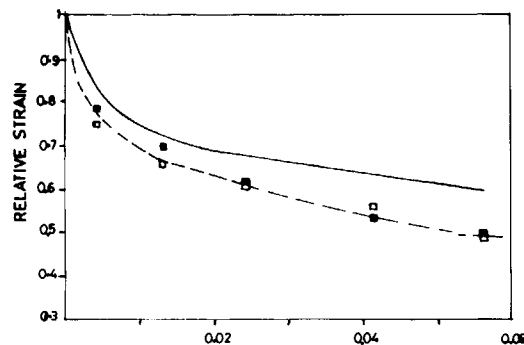


Figure 2 Variation of relative strain (ϵ_c/ϵ_p) of PP/Ag (open symbols untreated and closed symbols treated) composites with volume fraction of filler (ϕ_F). The solid curve represents the predicted behavior according to eq. (3). The dashed curve represents variation of data.

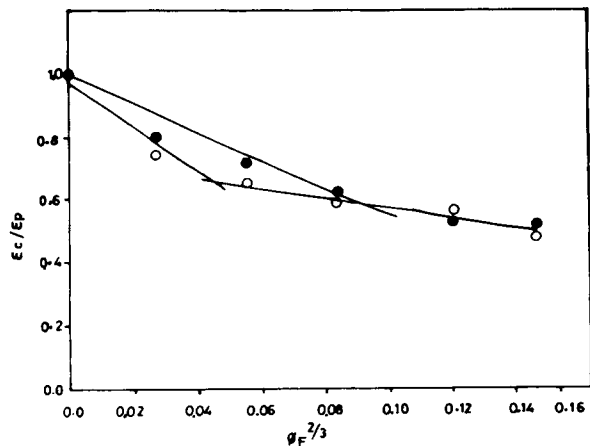


Figure 3 Variation of relative elongation at break (ϵ_c/ϵ_p) of PP/Ag (open symbols untreated and closed symbols treated) composites with filler area fraction $\phi_F^{2/3}$.

Ag particles as foreign matter or impurity. Surface treatment of filler improved modulus marginally (Fig. 1). This may be due to a marginally higher wettability of the filler with PP, which leads to improved dispersion of filler reducing filler agglomeration Figure 10.

If it is assumed that the Ag particles have no interaction with PP, these may be considered as voids or pores in the matrix so that the composite structure would resemble a plastic foam. The relative modulus of the foam was compared with some predictive theories¹⁰⁻¹² in Figure 1 using the following equations:

$$\frac{E_c}{E_p} = 1 - \phi_F^{2/3} \tag{1}$$

$$E_c/E_p = \frac{1 - \phi_F^{2/3}}{1 - \phi_F^{2/3} + \phi_F} \tag{2}$$

where the filler volume fraction can be assumed equivalent to the voids content. Equation (1) represents the upper bound curve A in Figure 1, whereas eq. (2) represents the lower bound curve B in Figure 1 for the relative modulus values. The experimental data fall far below these limits, implying a much larger extent of reduction of the value due to non-interacting Ag filler in PP as well as gross reduction of the crystallinity of iPP (Table I).

Elongation at break decreases with an increase in Ag content in the manner shown in Figure 2. The decrease is quite sharp by incorporation of a low volume percent of Ag ($\phi_F = 0.43\%$) and then the decrease becomes only marginal with further increase of Ag content. In metallic particle filled composites, generally sharp metal particles tend to create

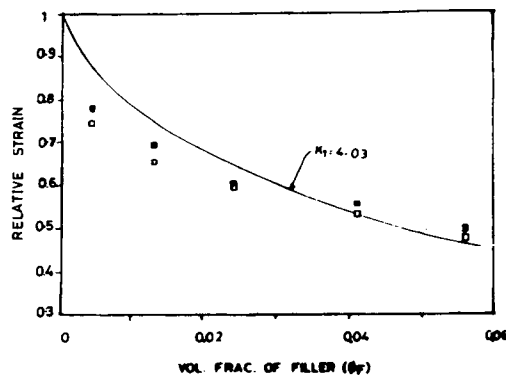


Figure 4 Variation of relative elongation at break (ϵ_c/ϵ_p) of PP/Ag (open symbols untreated and closed symbols treated) composites versus volume fraction of filler (ϕ_F). The solid curve represents the predicted behavior according to eq. (4) with K_1 value 4.03.

stress concentrations that initiate and propagate cracks. As a result, matrix deformation is reduced in some pseudologarithmic fashion with increasing filler content.

Assuming perfect adhesion,^{13,14} Nielsen¹⁴ calculated the elongation of the composites to the elongation of the unfilled specimen as

$$\epsilon_c/\epsilon_p = (1 - \phi_F^{1/3}) \tag{3}$$

The Nielsen model, eq. (3), lies far above the data (Fig. 2). This may be due to the nonadhesion of the Ag powder in the PP, which creates weak structures in the composites. Fillers interfere with the molecular mobility or deformability of PP matrix as well

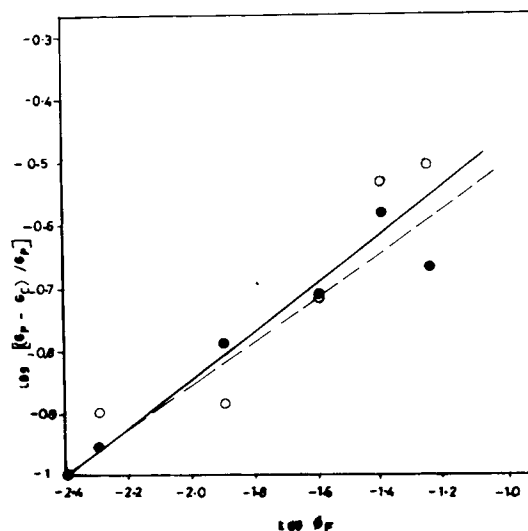


Figure 5 Plot of $\log[(\sigma_p - \sigma_c)/\sigma_c]$ of PP/Ag (open symbols untreated and closed symbols treated) composites versus $\log \phi_F$.

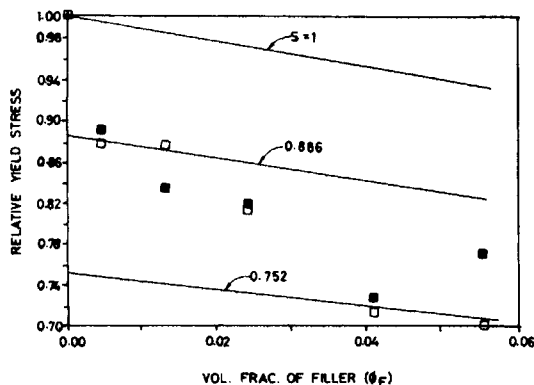


Figure 6 Variation of relative yield stress (σ_c/σ_p) of PP/Ag (open symbols untreated and closed symbols treated) composites versus ϕ_F . Solid curves represent predicted behavior according to eq. (7) with S values indicated.

as vacuole formation¹⁵ due to the dewetting or debonding of the polymer from the filler surface. Then the relative amount of void (i.e., the ratio between void and filler content) at break increases with an increase in filler content due to the crystalline nature of PP.¹⁵ In the composites with surface treated fillers, a plasticizing or lubricating type of behavior by the coupling agent is indicated, which reduces the deformability of PP to a lesser extent.

The decrease of elongation to lower values than the Nielsen model eq. (3) hints at a relationship of filler area fraction $\phi_F^{2/3}$ and elongation. Figure 3 shows a plot of ϵ_c/ϵ_p versus $\phi_F^{2/3}$ that reveals that the elongation is very sensitive to filler surface area up to $\phi_F^{2/3} = 0.046$ and the sensitivity is lowered with further increase in $\phi_F^{2/3}$. Filler surface modification decreases the sensitivity to a small extent.

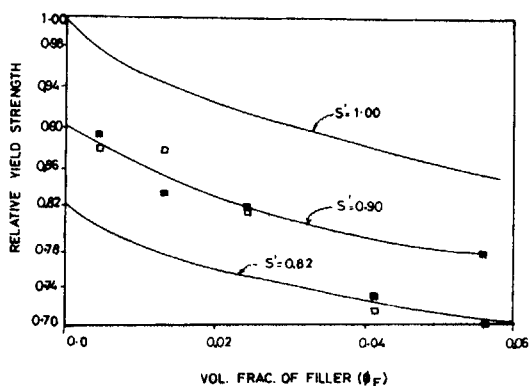


Figure 7 Plot of relative yield strength (σ_c/σ_p) of PP/Ag (open symbols untreated and closed symbols treated) composites versus volume fraction of filler (ϕ_F). Solid curves represent predicted behavior according to eq. (8) with S' values indicated.

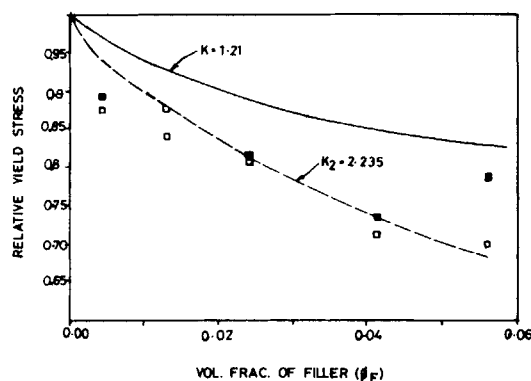


Figure 8 Plot of relative yield stress (σ_c/σ_p) of PP/Ag (open symbols untreated and closed symbols treated) composites versus volume fraction of filler (ϕ_F). Solid curves represent predicted behavior according to eq. (9) with $K_2 = 1.21$; dashed curves represents average variation of data.

The elongation data were treated according to a model described by Mitsubishi et al.⁸ to study the effect of filler polymer interaction:

$$\epsilon_c/\epsilon_{p_0} = (1 - K_1\phi_F^{2/3}) \quad (4)$$

where K_1 is a constant depending on filler size and the modification of fillers.

Following the method described by Mitsubishi et al.,⁸ the value of K_1 from eq. (4) was obtained and is presented in Table II. The mean value of K_1 estimated for the treated Ag-filled system was 4.32 and the untreated Ag-filled system was 4.62. The values of K_1 are quite high (2.32) for the untreated CaCO_3/PP system and 1.67 for the treated $\text{CaCO}_3/$

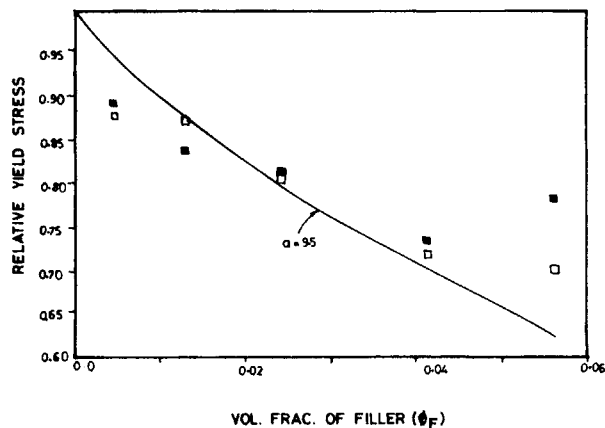


Figure 9 Variation of relative yield stress (σ_c/σ_p) of PP/Ag (open symbols untreated and closed symbols treated) composites versus volume fraction of filler (ϕ_F). Solid curves represent the predicted behavior according to eq. (10) with $\alpha = 9.5$.

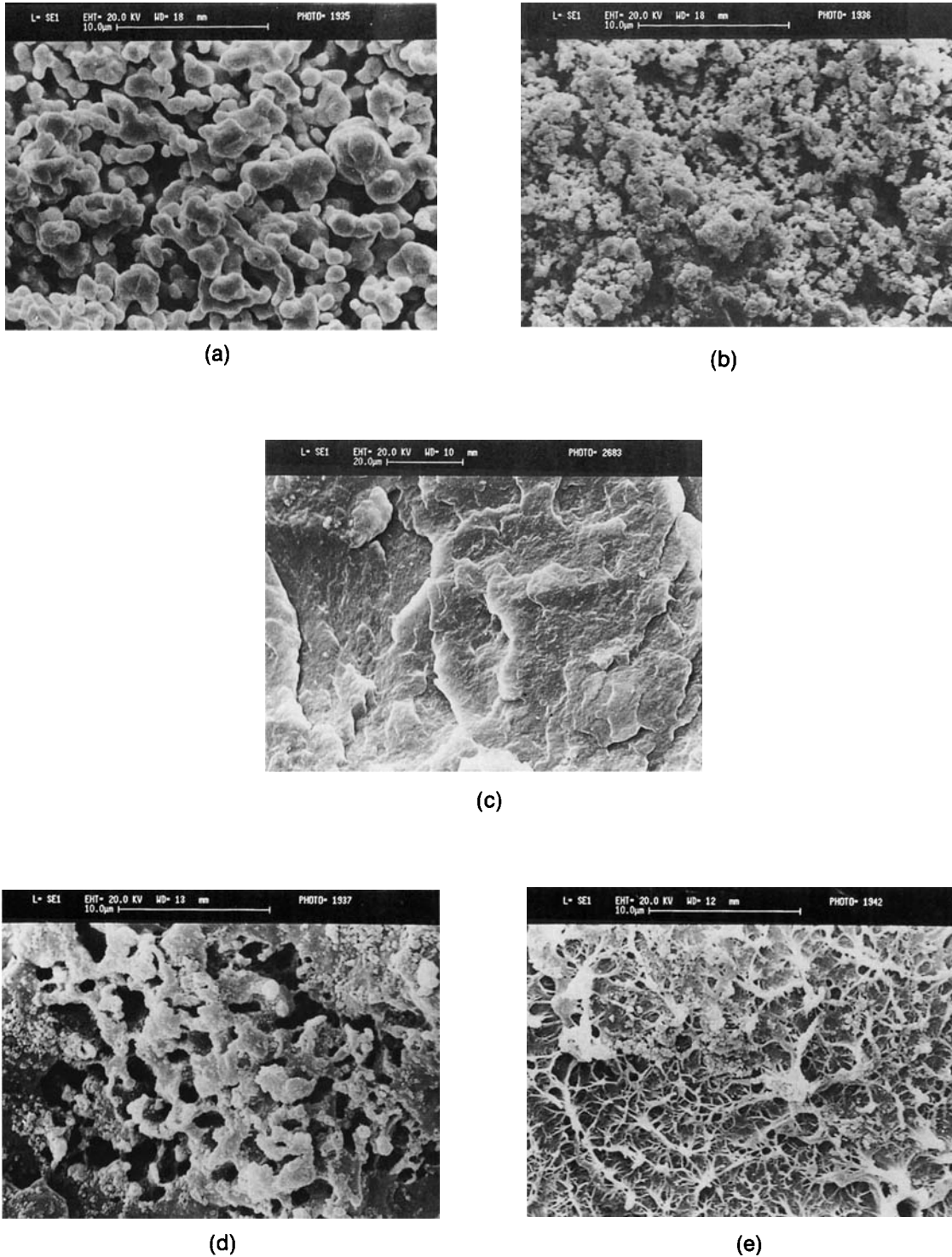


Figure 10 Scanning electron micrographs of (a) untreated Ag, (b) treated Ag, (c) PP and dispersion of Ag in PP, (d) PP/Ag 5.6 vol % untreated, and (e) PP/Ag 5.6 vol % treated.

PP system) compared to reported values for the PP/CaCO₃ system.¹⁶ This indicates a smaller degree of interaction between the phases.

The interaction parameter decreases for the surface treated composites revealing a plasticizing/lu-

bricating effect of the coupling agent. The curve shown in Figure 4 is for comparison of experimental data and model eq. (4).

The modulus and elongation data indicated that the addition of Ag powder into PP creates weak

Table I Values of Crystallinity of PP Components in PP/Ag Composites

Composite Composition	Crystallinity	
	DSC Method (J/G)	X-Ray Method (%)
PP	80.18	69
PP/Ag, 0.43%	67.22 (60.44)	61 (63)
PP/Ag, 1.3%	57.39 (67.65)	55 (62)
PP/Ag, 2.4%	46.11 (60.39)	59 (61)
PP/Ag, 4.1%	41.62 (58.57)	51 (53)
PP/Ag, 5.6%	44.57 (44.97)	50 (56)

The values in the parentheses are for PP/Ag (treated) composites.

structures in the composites. In the particulate filled composites debonding and dewetting of the polymer from the filler surface coupled with the agglomeration of filler particles create stress concentrations that in turn generate discontinuities in the structure, rendering it weak. For any significant contribution in mechanical and other properties by the inclusion in a two-phase composite, the inclusion is required to maintain continuity in the structure and/or interfacial adhesion with the matrix. Subsequent analysis of tensile stress data will shed more light onto these characteristics of the composites.

ANALYSIS OF TENSILE STRESS DATA

The tensile stress data were analyzed to understand the formation of the weak structure in these composites using some of the predictive models. The most common expressions of composition dependence of tensile stress of two-phase composites are based on the first power law, eq. (5), and the two-thirds power law, eq. (6), and expressed as

$$\frac{\sigma_c}{\sigma_p} = (1 - \phi_F) \quad (5)$$

$$\frac{\sigma_c}{\sigma_p} = (1 - \phi_F^{2/3}) \quad (6)$$

where σ_c and σ_p denote the tensile stress of the composite and matrix, respectively. The power laws originate from the relationship of area fraction and volume fraction of the inclusion.^{17,18} For a completely random distribution of the dispersed phase, the first power law relationship, and for the case of spherical inclusions the two-thirds power law with appropriate weightage factor, can be derived on simple mathe-

matical consideration. The following models were used:

$$\frac{\sigma_c}{\sigma_p} = (1 - \phi_F)S \quad (7)$$

$$\frac{\sigma_c}{\sigma_p} = (1 - \phi_F^{2/3})S' \quad (8)$$

$$\frac{\sigma_c}{\sigma_p} = (1 - K_2\phi_F^{2/3}) \quad (9)$$

$$\frac{\sigma_c}{\sigma_p} = \exp(-a\phi_F). \quad (10)$$

These equations describe the nonadhesion type structure.

In the first power law expression [eq. (7)] the parameter S accounts for the weakness in the structure introduced through discontinuity in stress transfer or formation of stress concentration points at the filler-polymer interphase, in analogy to the parameter S' in the Nielsen model¹⁸ [eq. (8)]. When the value S' (or S) is unity, "no stress concentration effect" is indicated, the lower the value of S' (or S) the greater the "stress concentration effect." The weightage factor K_2 in eq. (9) describes adhesion quality between the matrix and inclusion¹⁹ and depends on the details of the model, for example, $K = 1.1$ represents dense hexagonal packing in the plane of highest density, $K = 1.21$ describes the extreme case of poor adhesion¹⁷ with spherical inclusions for the minimum cross section between spherical beads, and $K = 1.0$ stands for strain consideration.¹⁸ In general, the lower the value of K below 1.21, the better the adhesion. According to the porosity model, eq. (10), the inclusion may be considered as pores or voids in polymer blends¹⁷ and composites²⁰ in analogy to the same in nonpolymeric materials such as metals and ceramics.²¹ The pores

Table II Values of Parameter K_1 [eq. (4)] in PP/Ag Composites

Ag Vol %	Values of K_1	
	PP/Ag	PP/Ag/LICA-38
0	—	—
0.43	9.511	8.356
1.3	6.232	5.576
2.4	4.779	4.779
4.1	3.940	3.761
5.6	3.541	3.444
Mean value	4.62	4.32

For K_1 the mean was for last four values, i.e., $\phi_F \geq 1.3\%$.

are assumed to not play any influential role on the mechanical properties of the composites as a result of nonadhesion at the interphase boundary. The parameter a describes¹⁷ stress concentration, the higher the value of a , the higher the stress concentration.

A plot of $\log[(\sigma_p - \sigma_c)/\sigma_p]$ versus $\log \phi_F$ from the tensile stress data, is exhibited in Figure 5 to estimate the suitability of the first or the two-thirds power law to the PP/Ag composites. From the slope of this plot the value of the power law exponents can be assigned according to eq. (7) or (8) in the absence of parameters S and S' . It may be noted that the slope was 0.81 (0.84 for treated Ag), which is closer to first power law than the two-thirds power law.

The first power law was shown to be better applicable than the fractional power law in the analysis of strength²² of composites. Further modification to the present analysis will be exhibited when the stress concentration parameters described in eqs. (7)–(10) are considered.

Some degrees of agreement could be reached between tensile stress data and first and fractional power laws as well as the Nicolais–Narkis¹⁹ and porosity model eqs. (7)–(10), by the use of suitable values of S , S' , K_2 , and a presented in Table III.

Comparison of tensile stress data with the predictive models are shown in Figures 6–9. It may be noted that according to the first and fractional power law models, the values of stress concentration parameters (S and S') were less than unity, indicating significant weakness or discontinuity in the structure. The Nicolais and Narkis model¹⁹ and the porosity model also exhibited similar results.

According to first power law model, eq. (7), the experimental data deviate from the theoretical curve with $S = 1$ (Fig. 6) and the S value from the experimental results lies between 0.89 and 0.75 indicating very high stress concentration points that increase with filler content. The Nielsen model, eq. (8), also

shows similar transition from no stress concentration ($S = 1$ in case of unfilled PP) to a moderate stress concentration level.

The experimental curve lies far below the theoretical curve ($S' = 1$, Fig. 7), indicating stress concentration. The stress concentration values lie between 0.90 and 0.82. According to the Nicolais and Narkis model,¹⁹ eq. (9), the theoretical curve predicted higher values (Fig. 8). A slight adjustment in the value of K_2 using 2.235 in place of 1.21, gives a closer fit with the experimental data. This may be attributed to the deviation of the system from the two-thirds power law due to nonconformity of the filler from the spherical shape.

Finally, experimental results showed somewhat better agreement with porosity [eq. (10)] with $a = 9.5$ as shown in Figure 9. It may be pointed out that the higher the value of a , the greater is the stress concentration. Therefore, these models also indicate the occurrence of significant stress concentration in the PP/Ag composites similar to other studies.¹⁵

Impact Strength

The dependence of the relative impact strength (ratio of the impact strength of the composites, I_c , to that of the unfilled polymer, I_p) I_c/I_p on volume fraction of the filler ϕ_F is presented in Figure 11. Notched impact strength decreases rapidly with addition of Ag filler and with the increasing Ag concentration. Addition of Ag $\phi_F = 0.43\%$ resulted in a sharp decrease in impact strength beyond which a gradual decrease was observed. The decrease of notched impact strength by addition of rigid filler is a general trend,¹⁵ because fillers in the composites (PP/Ag) remained in agglomerated form, which produced stress concentration points. The impact induced crack can readily propagate along the particle–polymer interface due to a noninteracting type of Ag

Table III Values of Stress Concentration Parameters S [eq. (7)], S' [eq. (8)], K_2 [eq. (9)], a [eq. (10)] in PP/Ag and PP/Ag/LICA-38 Composites

Ag Vol %	S	S'	K_2	a
0	—	—	—	—
0.43	0.8788 (0.8969)	0.8987 (0.9163)	4.735 (4.087)	31.05 (26.55)
1.3	0.8848 (0.8492)	0.9243 (0.8872)	2.2953 (2.9312)	10.42 (13.58)
2.4	0.7923 (0.8318)	0.8854 (0.8854)	2.2647 (2.265)	8.688 (8.688)
4.1	0.7446 (0.7670)	0.8104 (0.8348)	2.4066 (2.226)	8.213 (7.489)
5.6	0.7433 (0.336)	0.8219 (0.9216)	2.0404 (1.458)	6.326 (4.2796)
Mean value	0.8088 (0.8355)	0.8681 (0.8891)	2.2518 (2.2201)	8.412 (8.509)

The values in the parentheses are for PP/Ag/LICA-38 composites. For S and S' , the mean was taken for samples with $\phi_G \geq 0.43\%$. For K_2 and a the mean was for the last four values, i.e., for composites with Ag vol % ≥ 1.3 .

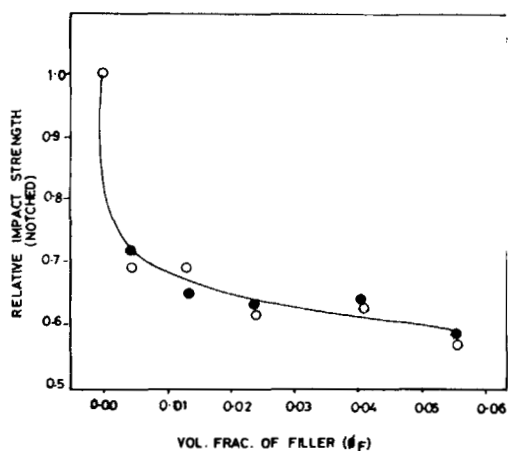


Figure 11 Variation of relative notched Izod impact strength with volume fraction of filler (ϕ_F) of PP/Ag (open symbols untreated and closed symbols treated) composites.

particles in the PP matrix. The PP/Ag composites form a weak discontinuous structure.

LICA-38 treated Ag/PP composites also exhibited a similar trend: the impact values are slightly higher or similar to the untreated Ag-filled compositions. This may be due to a degree of better dispersion of Ag particles and the plasticizing/lubricating effect of coupling agent.²³ The impact strength decreases with the formation of stress concentration points at higher Ag content.

Flexural Properties

The variation of relative flexural modulus (E_{Fc}/E_{Fp}) and flexural strength (σ_{Fc}/σ_{Fp}) of the composites are presented in Figures 12 and 13 as function of ϕ_F . Flexural modulus and strength increased steadily with Ag content.

iPP is a hydrocarbon polymer having a very low level of intermolecular interaction forces. Fortunately, the polymer molecule fits into a helical type of crystal structure that essentially accounts for its mechanical strength.²⁴ Incorporation of any foreign inclusions such as filler would interfere with the crystallization, reducing in the process the strength properties. The strength of the polymer may be retained if the loss of crystallinity is compensated for by increased interfacial interaction of iPP with the inclusion. Thus polymer inclusion interphase¹³ plays much important role in determining the strength property of PP-based composites.

It was already observed that in the Ag-filled iPP composites the tensile modulus, strength, and breaking elongation decreased with Ag content. In fact, Ag particles were not bonded with PP and this debonding was observed during tensile testing in the

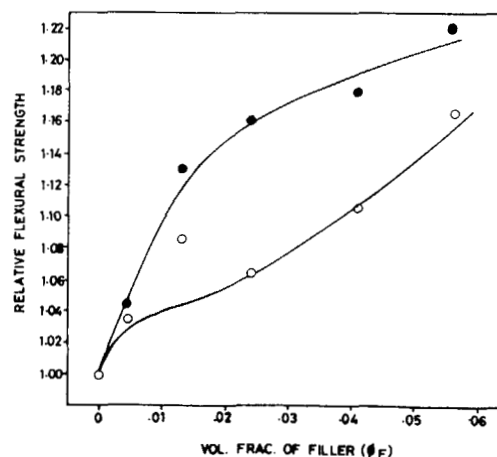


Figure 12 Variation of relative flexural strength with volume fraction of filler (ϕ_F) of PP/Ag (open symbols untreated and closed symbols treated) composites.

form of whitening of the samples (due to light scattering) near the breaking area prior to failure. Debonding of filler from the iPP matrix could cause a large decrease in tensile modulus and strength.¹³ Furthermore, presence of Ag decreased the crystallinity of iPP, as shown by X-ray diffraction and DSC studies (Table I), that in turn decreased the strength properties. Hence the absence of interaction of iPP and Ag and loss of crystallinity decreased the tensile strength and modulus. The elongation decreased due to an increase in rigidity of PP in the presence of filler.

It is interesting to note that with Ag filler, although tensile modulus and strength decreased,

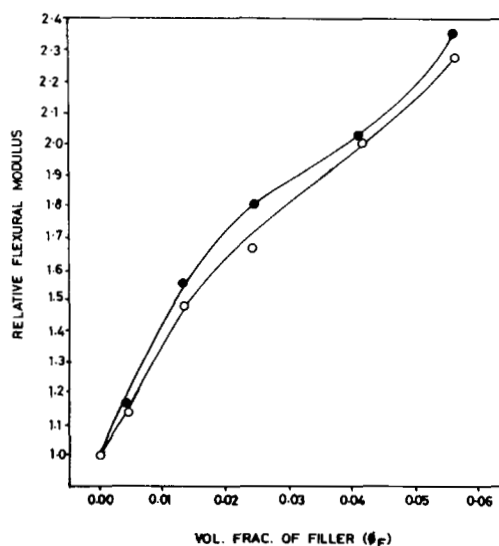


Figure 13 Variation of relative flexural modulus with volume fraction of filler (ϕ_F) of PP/Ag (open symbols untreated and closed symbols treated) composites.

flexural modulus and strength increased with Ag content. It is well known that in the three point bending type of flexural test that was performed in this work, the loaded surface undergoes compression while the surface on the opposite side undergoes tension.¹⁴ It is also well known that in tension any flaw or defect in the composite body will magnify, whereas in compression the defect will not weaken the structure but will be plugged.²⁵ Because the flexural tests were performed at low deformation (5% strain), it is possible that in these composites the weakness in the structure does not have time to take effect, so the body displays rigidity in bending. The predominance of the compressive component of the bending stress relative to its tensile counterpart may be the reason for this rigidity. This happens because Ag powders are rigid and incompressible particles, when added to PP matrix, leave a reduced degree of room for compressive deformation of PP. The rigidity of the composites is thus due to the increased restriction of molecular deformation of PP by rigid incompressible Ag fillers. The rigidity increases with the filler content so that flexural modulus and strength also show an increasing trend. Similar results were reported^{15,25} in other systems also.

CONCLUSION

Incorporation of Ag particles greatly modifies the mechanical properties of iPP. Tensile modulus, strength, and breaking elongation decreased with increase in Ag concentration. The composites form a discontinuous structure on addition of Ag particles. Ag particles create stress concentration or weak points on the PP matrix that initiated and propagated cracks lowering the values. Izod impact strength decreased with incorporation of filler. Ag particles, creating stress concentration points in the structure, readily facilitated the propagation of an impact induced crack along the particle-polymer interface due to the noninteracting type of Ag particles in the PP matrix.

Flexural strength and modulus both increased with Ag content. This is because rigid and incompressible silver powders do not leave sufficient space for compressive deformation of PP to take effect.

Surface treatment of filler shows marginally improved mechanical properties that may be due to a higher degree of wettability of the filler with PP,

facilitating filler dispersion in the matrix by reducing filler agglomeration.

REFERENCES

1. T. A. Skotheim, Ed., *Handbook of Conductive Polymers*, Vol. 1, Marcel Dekker, New York, 1986.
2. D. M. Bigg, *Polym. Compos.*, **7**, 125 (1986).
3. J. M. Margolis, Ed., *Conductive Polymers and Plastics*, Chapman and Hall, New York, 1989.
4. H. Katz and J. V. Milewski, Eds., *Handbook of Fillers for Plastics*, Van Nostrand Reinhold, New York, 1978, Sect. IV.
5. M. Arroyo, F. Perez, and J. P. Vigo, *Polym. Compos.*, **7**, 6 (1986).
6. D. R. Saini, A. V. Shivoy, and V. M. Nadkarni, *Polym. Eng. Sci.*, **13**, 807 (1985).
7. S. J. Monte and G. Sugerman, KEN-REACT Reference Manual, Bulletin No. KR-1084 L, 1985.
8. K. Mitsuishi, S. Kodama, and H. Kawasaki, *Polym. Eng. Sci.*, **25**, 1069 (1985).
9. E. P. Plueddemann, in *Interfaces in Polymer Matrix Composites*, E. P. Plueddemann, Ed., Academic, New York, 1974, Chap. 6.
10. L. J. Cohen and O. Ishai, *J. Compos. Mater.*, **1**, 390 (1967).
11. O. Ishai, disc of article by U. J. Counto, *Magn. Concr. Res.*, **17**, 148 (1965).
12. B. Paul, *Trans. AIME*, **36**, 218 (1960).
13. J. A. Manson and L. H. Sperling, *Polymer Blends and Composites*, Plenum, New York, 1976, Chap. 12.
14. L. E. Nielsen, *Mechanical Properties of Polymers and Composites*, Vol. 2, Dekker, New York, 1974, Chap. 7.
15. S. N. Maiti and P. K. Mahapatro, *Poly. Plast. Technol. Eng.*, **30**, 559 (1991).
16. S. N. Maiti and P. K. Mahapatro, *J. Appl. Polym. Sci.*, **42**, 3101 (1991).
17. T. Kunori and P. H. Geil, *J. Macromol. Sci. Phys.*, **B18**, 135 (1980).
18. L. E. Nielsen, *J. Appl. Polym. Sci.*, **10**, 97 (1966).
19. L. Nicolais and M. Narkis, *Polym. Eng. Sci.*, **11**, 194 (1971).
20. L. E. Nielsen, *J. Compos. Mater.*, **1**, 100 (1967).
21. E. M. Passmore, R. M. Spriggs, and T. Vasilos, *J. Am. Ceram. Soc.*, **48**, 1 (1965).
22. S. Sahu and L. J. Broutman, *Polym. Eng. Sci.*, **12**, 91 (1972).
23. C. D. Han, T. Van Den Weghe, P. Shete, and J. R. Haw, *Polym. Eng. Sci.*, **21** (4), 196 (1981).
24. J. A. Brydson, *Plastics Materials*, 5th ed., Newnes Butterworths, London (1989).
25. S. N. Maiti and P. K. Mahapatro, *Polym. Compos.*, **11**, 223 (1990).

Received December 28, 1994

Accepted September 30, 1995